


Review

Overview of Observed Clausius-Clapeyron Scaling of Extreme Precipitation in Midlatitudes

Marta Martinkova ^{1,2,*}  and Jan Kysely ^{1,2}

¹ Institute of Atmospheric Physics, Czech Academy of Sciences, 14100 Prague 4, Czech Republic; kysely@ufa.cas.cz

² Faculty of Environmental Sciences, Czech University of Life Sciences Prague, Kamýcká 129, 16500 Praha-Suchbát, Czech Republic

* Correspondence: marta@ufa.cas.cz

Received: 30 May 2020; Accepted: 22 July 2020; Published: 25 July 2020

Abstract: This paper presents an overview of recent observational studies on the Clausius-Clapeyron precipitation-temperature (P-T) scaling in midlatitudes. As the capacity of air to hold moisture increases in connection with increasing temperature, extreme precipitation events may become more abundant and intense. The capacity of air to hold moisture is governed by the Clausius-Clapeyron (CC) relation, approximately 7% per °C. Departures from this, so called super-CC scaling and sub-CC scaling, are consequences of different factors (moisture availability, type of precipitation, annual cycle, the percentile of precipitation intensity and regional weather patterns). Since the moisture availability and enhanced convection were considered as the most important drivers governing the P-T scaling, dew point temperature as a scaling variable is discussed in detail and methods of disaggregation of precipitation events into convective and non-convective are also reviewed.

Keywords: Clausius-Clapeyron scaling; precipitation extremes; midlatitudes

1. Introduction

The capacity of air to hold moisture increases with increasing temperature and extreme precipitation events are generally expected to become more intense and frequent due to the global warming [1–3]. The most extreme events occur when almost all of the moisture contained by the volume of air is precipitated and, consequently, they are expected to be more intense with more available moisture [4]. This hypothesis was initially established on theoretical grounds [5,6], then it was supported and validated by climate models simulations, e.g., [7–16] and by observational studies, e.g., [9,17–20].

Globally, surface evaporation that is enhanced by global warming mainly over the oceans is a driver for increased precipitation. In other words, global precipitation increases with warming and decreases with cooling [21]. Increases in global mean precipitation are constrained by changes in the net radiative cooling rate of the troposphere; according to the recent outputs of global climate models, it lies within a range of 1% to 3% per °C [1,22–24]. Thus, the increasing temperature leads to the intensification of the global hydrological cycle [1] with important potential consequences, including observed enhanced hydrological extremes [25–28], as extreme precipitation events often lead to flooding [29].

The rate of change of saturated water vapor pressure with temperature is described by the Clausius–Clapeyron (CC) relation. The approximate value of the change is 7% per °C. On the local or regional scale, the CC relation determines the rate of change in intensity of extreme precipitation events in the case of absence of other factors, e.g., changes in circulation patterns (a dynamical factor) and in moisture content (a thermodynamic factor) [6,24,30].

It has been observed that subdaily precipitation extremes are more sensitive to changes in temperature than the ones on a daily timescale, recently e.g., [31]. The “super-CC” relation, i.e., an increase higher than 7%, was first identified in daily and hourly records from a single station in the Netherlands [32]. Since then, many studies evaluated the scaling between extreme precipitation and temperature in a wide range of spatial and temporal scales in various climate settings, e.g., [33–38].

The overall goal of these studies is to identify the value of scaling, find its drivers, and explain the observed scaling to assess local precipitation conditions. The super-CC scaling is interpreted in connection with convective precipitation [39]. This is highly relevant for midlatitudes in the warm part of the year when convective precipitation represents important part of total amounts. Further, the increase in convective precipitation was reported by observational studies in midlatitudes [40–44]. Additionally, according to [45,46] the most considerable increases are probable for sub-daily precipitation events. Hence, higher frequency and bigger magnitude of flash floods may also be expected due to increasing temperature.

As the type of precipitation is one of the most important factors governing the precipitation-temperature (P-T) scaling, the classification of precipitation into the stratiform (non-convective) and convective components is beneficial while studying the P-T scaling. Stratiform precipitation is large-scale precipitation from stratiform clouds (e.g., nimbostratus). The stratiform precipitation is usually long-lasting and it has smaller intensity. Its precipitation particles are smaller. On the other hand, convective precipitation is associated with convective clouds (e.g., cumulonimbus). Most often, it occurs as rain showers and thunderstorms of a relatively small spatial extent. Its precipitation particles may grow to large sizes [47]. The importance of regional studies is highlighted by the large spatial variability of convective extremes.

The main objective of this paper is to provide an overview of the results of recent observational studies in midlatitudes, especially those that are not covered by the review published in 2014 by Westra et al. [45]. The overview is focused on different methodological approaches (data selection, scaling methods, event classifications and differentiations of convective and stratiform events).

This work is organized, as follows: firstly, the theoretical background of the Clausius–Clapeyron relation is provided. Subsequently, the P-T scaling identified by observational studies in midlatitudes is discussed with a focus on the interpretation of departures from the CC scaling. Special attention is paid to the role of convective precipitation and overall moisture availability. The last section of the paper summarizes the methods and data sets used in the assessment of the P-T scaling and the methods for the disaggregation of convective and non-convective precipitation are also reviewed due to the important role of convective precipitation in the super-CC scaling.

2. Clausius–Clapeyron Relation

The Clausius–Clapeyron equation characterizes a phase transition between two phases of the matter of a single component. On the pressure-temperature diagram, it delineates the slope of the coexistence curve (1) :

$$\frac{dP}{dT_K} = \frac{L}{T_K \Delta v} = \frac{\Delta s}{\Delta v} \quad (1)$$

where P denotes pressure, T_K temperature (in Kelvin), L specific latent heat, v specific volume, and s denotes specific entropy.

Regarding the capacity of the atmosphere to hold moisture, the CC equation can be rewritten in the form [45]:

$$\frac{\delta e_s}{\delta T_K} = \frac{L_v e_s}{R_v T_K^2} \quad (2)$$

where e_s is saturation water vapor pressure, L_v is the latent heat of vaporization, and R_v is the gas constant.

The empirical form of equation (2) relates e_s to local air temperature T (in °C) in a nearly exponential rate [48]:

$$e_s = 6.1094e^{\frac{17.625T}{T+243.04}} \quad (3)$$

The formula is usually further approximated as a rate of 7% per °C with an assumption that all factors influencing precipitation but temperature remain constant and, consequently, precipitation will be proportional to the amount of water that is held in the atmosphere. Moreover, the rate of change of e_s with T may also be the rate of change for the most intense precipitation events with T [5].

3. Precipitation-Temperature Scaling Identified by Observational Studies

P-T scaling observational studies cover a wide range of climate conditions and different spatial and temporal scales. They can be categorized into studies that consider local temperature and studies considering temperature change with global warming.

Several prevailing features were reported: the approximate CC rate of 7% per °C was identified for temperatures up to 12 °C, the P-T scaling up to triple this rate was observed for temperatures up to 24 °C and decrease of the P-T scaling or a negative P-T scaling was detected for temperatures above 24 °C [45,49]. Interestingly, similar behavior was reported from Paleocene–Eocene Thermal Maximum (56 Ma) strata in Spain: the super-CC scaling was identified above 12 °C while a decrease of precipitation intensity was found above 24 °C [50].

Generally, the resulting P-T scaling can be influenced by processes that are not necessarily purely thermodynamic. Consequently, the general term P-T scaling is used here for any scaling between precipitation and temperature identified in observational studies. The following terms are used for approximate quantification of the P-T scaling following the usual practice: sub-CC scaling (less than 7%), CC scaling (approximately 7%), super-CC scaling (more than 7%), and 2CC scaling (approximately 14%). The term negative scaling refers to the case when precipitation decreases with temperature.

This section is organized, as follows: firstly, the variables used for analysis of the P-T scaling are described, then the results of observational studies regarding the increase in the P-T scaling above CC are discussed and summarized, and finally the drivers of the decreased P-T scaling at higher temperatures are discussed.

3.1. Variables Used for Analysis of the P-T Scaling

Regarding precipitation, most observational studies use high percentiles of 1-h intensities for the assessment of the P-T scaling, because they represent extreme precipitation events better than daily intensities. Subhourly intensities are identified to be even more sensitive to temperature than hourly intensities [31,33]. However, some studies found opposite behavior [51]. The probable explanation for these generally heterogeneous results could be that precipitation extremes are, besides other important factors, heavily influenced by intermittency, as shown by a modeling study [52].

The most often used temperature variable is the daily mean temperature. The motivation is that it represents the temperature of the air mass better than the hourly temperature that is influenced by boundary-layer processes and radiation [32]. Nevertheless, the hourly temperature was successfully tested for the P-T scaling with very similar results to the daily temperature [53]. Moreover, the P-T scaling of daily and hourly temperature was compared in a study in the contiguous US with similar results [54].

The P-T scaling while using surface temperature is only robust under the assumption that relative humidity remains constant [55]. To avoid this limitation, the dew point temperature (temperature at which the air becomes saturated with water vapor at constant pressure) prior to the precipitation event is used instead of surface temperature [49,56,57]. The motivation is the underrepresentation of the highest temperatures in the data set because of the cooling by precipitation. This issue can also be addressed by using temperature of condensation level instead of surface temperature [34,53]. Some of the observational studies carried out the analysis of the relationship between the extreme precipitation and both the surface air and dew point temperature in order to evaluate whether temperature influence on extreme precipitation is an issue of moisture availability, e.g., [31,35,51,58].

In Austria, for example, moderate intensities showed higher sensitivity to dew point temperature than to the surface temperature, however, results for high percentiles were not significantly different between surface temperature and dew point temperature [31]. The definitions of moisture-limiting threshold temperatures were proposed as an alternative to using precipitation—dew point temperature relations to identify moisture limitations [51]. Another approach for the assessment of the role of available moisture in the P-T scaling was used in an observational study in China; the tripole relation among surface temperature, atmospheric moisture, and precipitation was investigated with heterogeneous results in midlatitudes [59].

Convective Available Potential Energy (CAPE) is also sometimes considered in studies on the P-T scaling. It is the total energy available for conversion to kinetic energy and it equals the total work that upward positive buoyancy force performs [60]. CAPE controls the maximum velocity of an adiabatically ascending positively buoyant air parcel and it increases as the air temperature rises [54,61]. For instance, heating and moistening near the surface, cooling high up in the troposphere, and release of additional latent heat during condensation [6] generates CAPE. Under idealized conditions, the fraction of CAPE transformed into kinetic energy, is constant. Subsequently, the vertical velocity of an ascending air parcel and, consequently, the condensation rate and intensity of rainfall are proportional to the square root of CAPE [62]. CAPE and dew point temperature were used as scaling variables in [54,62] to separate the effects of temperature on rainfall extremes via increased water content and via enhanced atmospheric convection.

The following factors were identified by the relevant literature as influencing the shape of the P-T scaling, e.g., [31,35,63]: type of precipitation, annual cycle, the percentile of precipitation intensity, regional weather patterns, including related different moisture availability in regions [64], pressure level of scaling temperature (surface vs. cloud temperature) [53], small and large-scale atmospheric dynamics, vertical stability, and CAPE feedbacks that might enhance convection. Clearly, most of these factors are strongly interconnected.

3.2. Increase of the P-T Scaling and Super-CC Scaling

Table 1 presents examples of P-T scaling observational studies with identified threshold temperature (THR) between CC (or sub-CC) and super-CC scaling. The P-T scaling that was distinctively steeper than the CC scaling was initially detected for station De Bilt, the Netherlands in the aforementioned study [32]. They identified the scaling between the 99th and higher percentiles of hourly precipitation and the daily temperature to be at approximately the CC rate of 7% per °C for temperatures up to 12 °C (in annual data) and approximately double this rate for temperatures up to 22 °C.

Table 1. Increase of the precipitation-temperature scaling identified by selected observational studies in midlatitudes and corresponding threshold temperature (THR). Where not stated explicitly the results are for the whole year and total precipitation.

Localization	Type/Season	Temperature	Precipitation	Percentile	below THR	THR	above THR
De Bilt, the Netherlands [32]	–	T daily	1-h	99%, 99.9%	≈7%	12 °C	≈14%
	–	T daily	1-h max	99%, 99.9%	≈7%	12 °C	≈14%
Four sites in W Europe [65]	–	Tdew	1-h	90%, 99%, 99.9%	≈7%	10 °C	≈14%, ≈17%, ≈17%
	–	T daily	1-h	99%, 99.9%	≈7%	10 °C	≈14%
Germany [33]	conv.	T daily	1-h	75%, 99%	≈7%	10 °C	above 7%
	total	T daily	1-h	75%, 99%	≈7%	12 °C	above 7%
the Netherlands [39]	conv.	Tdew	1-h max	above 50%		14%	
Vienna, Austria [53]	–	T hourly	1-h	90%,95%,99%	below 7%	12 °C	≈14%
	–	T hourly 700–500 hPa	1-h	90%,95%	below 7%	–10 °C	above 7%
	–	T hourly 700–500 hPa	1-h	99%		7% for the whole range	
Romania [66]	–	T daily	1-h	99%,	≈7%	10 °C	≈14%
	–	T daily	1-h	99.9%	≈14%	10 °C	≈14%
					for some stations		
United Kingdom [67]	spring	T daily	1-h	99%	below 7%	10 °C	above 7%
	summer	T daily	1-h	99%	below 7%	15 °C	above 7%
Sicily [63,68]	wet	T daily	30 min, 60 min	99%	below 7%	10–15 °C	above 7%
	dry	T daily	30 min, 60 min	99%	below 7%	10–15 °C	above 7%

The super-CC scaling was interpreted as being caused by dynamical feedbacks as a result of excess latent heat release in extreme showers [69]. The increasing temperature leads to increasing moisture content and more latent heat being released during condensation supports enhanced convection. Testing this hypothesis, the 2CC scaling of dew point temperature and hourly convective precipitation was linked to large-scale atmospheric conditions [39]. The spatial extent of a precipitation event was found to increase with increasing dew point temperature. Furthermore, the 2CC scaling was explained by enhanced convection due to an increase in near-surface humidity.

The size of a cloud cell can be a critical factor for the observed super-CC scaling of convective precipitation. The study [70] investigated the size and intensity of convective rain cells by tracking rainfall events in high-resolution radar data and found that higher intensities were accompanied by larger rainfall areas and larger events were more likely a result of the merging of rain cells. This was even more pronounced for dew point temperatures above 15 °C, where the size of events increased steeply. Microphysical processes probably also contribute to the observed super-CC scaling: precipitation extremes were identified to be sensitive to the fall speed of hydrometeors as different P-T scaling was obtained with different microphysics schemes in a modeling study [71].

The findings of the original study [32] were later extended with analysis of scaling conducted separately for convective and non-convective precipitation events and the super-CC scaling has been explained by the coexistence of the stratiform and convective types of precipitation at higher temperatures [72,73]. Then, in [56], the dew point temperature was taken 0, 2 and 4 h prior to the precipitation event and 14% scaling was identified for the dew point temperature measured 4 h before the event. This confirmed the large dependency of hourly precipitation extremes on near surface humidity and the super-CC scaling hypothesis. In the following studies, the high P-T scaling rates were explained by the shift from stratiform to convective precipitation and intensification of the convective precipitation [33,74–76].

The super-CC scaling was identified for convective events by most of the studies that distinguished between convective and stratiform (large-scale) precipitation, e.g., [31,51,54,73,77] and studies listed in Table 1. The observation that convective events can produce intensity increasing above the CC scaling was also endorsed by modeling studies [75,78]. On the other hand, intensities that are connected to stratiform precipitation often increase at approximately the CC rate, even at higher temperatures, e.g., [33,54].

The annual cycle has an important role in determining the P-T scaling [79] in case the different processes that drive extreme rainfall are dependent on the season. In the United Kingdom, consistent sub-CC scaling was observed in autumn and winter. In contrast, the super-CC scaling was identified for spring and summer [67]. The study proposed two explanations for the super-CC scaling: transition from the dominance of large-scale to localized convective rain or as a consequence of quasi-stationary convective storms.

In Sicily, the increase in the P-T scaling with temperature was identified for both dry and wet seasons (Table 1) and put in the connection with a transient period between the two seasons during which both convective and stratiform precipitation occur. Thus the observed P-T scaling can be interpreted as a result of coexistence of the two precipitation types [33].

In Romania, the P-T scaling was initially explored for the whole year and the P-T scaling close to CC was reported for the 90th percentile of hourly precipitation and close to 2CC for the 99th and the 99.9th percentiles between 10 °C and 22 °C.

The study [35] analyzed the P-T scaling of maximum daily rainfall intensities for durations ranging from 5 min to 12 h from station data in Canada with the following results: for short durations, the P-T scaling was close to CC in coastal regions while the super-CC with upper limit was observed in inland regions. The estimated P-T scaling was not sensitive to the percentile for sufficiently high percentiles. Interestingly, in contrast to the studies from Europe, the shape of the P-T scaling did not depend on season.

The influence of regional weather patterns was assessed by an observational study that was conducted in Austria [31]. They identified the P-T scaling to be lower in the mountainous western region than in the eastern lowlands. This was explained by different weather patterns that generate extreme precipitation in the two regions, as local topographic conditions may determine the P-T scaling [80]. Specifically, in the warmer eastern lowlands, the extreme precipitation is associated with short, convective rainfall events during summer and low gradient synoptic conditions with high shares of locally recycled moisture. In the mountainous western region, the extreme precipitation is sourced by Mediterranean moisture and local temperatures might be less indicative of the sensitivity. The cooling effect of large precipitation events, the orographic amplification of precipitation, and generally cooler temperatures in the Alpine environment may influence the P-T scaling. Because of the regional and seasonal variability of the precipitation intensities, a smaller ratio of the scaling can signify a bigger absolute change in intensity. For example, steep P-T scaling at low daily temperatures may not indicate large absolute changes in precipitation intensity and relatively less steep P-T scaling at high daily temperatures may have important consequences in terms of accumulated rain.

3.3. Decrease of the P-T Scaling at Higher Temperatures

Intensities of extreme precipitation may decrease above high temperature thresholds. This peak-like or hook-like structure was described as typical for the midlatitudes in a global study of the P-T scaling [81]. The threshold temperatures varied among different regions and they were interpreted to indicate a transition from a moist to a dry regime where a further intensification of rain is halted, as also reported by modeling studies, e.g., [82,83].

To illustrate the differences in threshold, daily temperatures among different regions, the following examples of recent observational studies in Europe are presented: for the French Mediterranean region, 15 °C has been described as a threshold temperature between the CC scaling and the sub-CC or negative scaling. This was explained by the dynamical contribution of orography [84]. In Sicily, the negative CC scaling was identified above 22 °C for the 99.9% percentile for the annual period and for the dry season (April–September). On the other hand, the decline in the P-T scaling was not identified for the wet season [63]. In Romania, the 99th and the 99.9th percentiles exhibited the negative scaling rates for temperatures above 22 °C [66,85]. Threshold temperature between the positive and negative scaling of convective 6-h precipitation was identified to equal 17 °C in the Czech Republic [76]. Similarly in Austria [86], both lowland and mountainous regions, for which the P-T scaling was compared, have threshold temperature around 17 °C. These findings suggest that in midlatitudes the threshold temperatures are higher in warmer regions. However, more results especially outside Europe are needed for such conclusion.

A study from a single station in Austria analyzed the P-T scaling between precipitation and the mean temperature at the hour of precipitation, daily mean temperature and the start of the precipitation accumulation period. The study identified a threshold temperature of P-T scaling stagnation around 19 °C for all three temperature variables within the range of temperature bins that contained enough data [53]. Mean temperature between the 700 and 500 hPa layers (cloud temperature) from a reanalysis was also tested by the study. For the cloud temperatures, the scaling remained constant over the whole temperature range for the 99th percentile (Table 1); sample sizes at the very warm end were larger for this percentile and, therefore, the results were more robust.

The aforementioned lack of moisture as a reason for the negative scaling at higher temperatures was discussed in [87]. The study argued that this can be an artifact originating from sample size when smaller samples underestimate high quantiles, and proposed the use of parametric quantile estimates from the generalized Pareto distribution fitted with L moments to remove this effect. The bin shifting mechanism was also proposed as a possible cause of the negative scaling at high temperatures based on the observation of daily extreme precipitation associated with local cooling.

4. Data Sets and Methods Used

Table 2 presents the overview of different methods and data sets used for assessment of the P-T scaling in midlatitudes. The particular data sets, including the quality checks and methods for assessment of the P-T scaling, apparently have an important impact on obtained results. For instance, operational gauge networks may underrate extreme convective precipitation over small areas [86] and further influence the estimated P-T scaling. Most of the regional studies are based on station or gridded observational data [31,51,54,63,67]. On the other hand, high resolution radar data were used for the analysis of the size and intensity of rain cells [70].

4.1. Methods to Depict the P-T Scaling

Most of the observational studies use the binning method in different versions and modifications (for example, see Table 2). The binning method is based on placing the temperature data into a fixed number of temperature bins with width from usually 1 °C to 3 °C. Subsequently, precipitation percentiles of interest are calculated for each bin. Some studies used the whole range of precipitation mboxcitemanola2018future, grillakis2018hydrometeorological; most of them included only events equal or above certain threshold, e.g., 0.1 mm per hour [32], 0.6 mm per hour [70], or 1 mm per hour [53]. Alternatively, the bins are defined in such a way that they have an equal number of precipitation observations, e.g., [63,88,89].

The small number of observations per bin may cause a decrease in the P-T scaling or even negative scaling [53]. Similarly, the smaller number of observations in a bin [90] may be the reason for the steeper P-T scaling than in the case when the number of observations per bin is higher [54,62]; the three studies were carried out for the same region and the latter two differed in that [62] was based on station data, while [54] on gridded station data.

As an alternative to the binning method, some studies fitted the quantile regression model to obtain more detailed information on the influence of temperature on precipitation intensity (see Table 2). Quantile regression method is also assumed to be more robust against outliers than the binning method [31,91].

The scaling function is usually analyzed for the linear trend to identify the scaling rate. Some other studies used different methods to detect the threshold temperature, e.g., LOESS interpolation and other examples in Table 2. A comprehensive comparison of three regression models (exponential regression, two-segment piece-wise regression, and LOESS regression) was carried out in the study for Sicily, where innovative use of piecewise and locally-weighted scatter plot smoothing regression-based approaches provided better insight into the P-T scaling, especially in the dry season [63].

Table 2. Overview of methods and data sets used by precipitation-temperature observational studies in midlatitudes.

Localization	Observational Period	Precipitation Data	Temperature Data	Scaling Method	Other data
UK [67]	1992–2011	1-h more than 1300 stations gridded data set	T daily	binning [88]	daily atmospheric circulation indices [92]
Netherlands [39]	1995–2014	P 1-h at 30 stations	T 1-h, Tdew 1-h	binning	1-h humidity
Netherlands [70]	2008–2016	5 min 1 km radar data	Tdew 1-h from stations rainfall events	binning with constant bin widths binning with constant bin numbers binning 2 °C overlap	
Netherlands [74]	8 years 16 years 16 years	P 10-min P 1-h P daily only wet intervals P 10 min	Tdew 1-h Tdew daily		
Switzerland [51]	1981–2011		T daily	quantile regression	rel. humidity lightning
Germany [93]	shortest 1971–1976 longest 1971–1987	5 stations 5 min resolution	T 1-h	binning 5 °C, overlap	3-h synop
SW Germany [33]	1997–2004 2007–2008	obrometers 90 stations 5 min resolution radar	T daily e-obs data set	binning 1 °C	3-h synop
Vienna, Austria [53]	1979–2011	P 1-h at 1 station	T 1-h	binning	ERA-Interim 1979–2011
Austrian SE Alpine foreland [31]	1958–2014	P 10 min., P 1-h rainfall events	T daily, Tdew daily gridded data set	quantile regression	circulation type classification ERA-Interim data 1979–2016
Medit. France [84]	1989–2008	P 3-h at 220 stations P 3-h SAFRAN analysis system	T 3-h at 220 stations T 3-h SAFRAN analysis system	binning [88]	atmospheric integrated water vapor
Mediterranean [94]	shortest 1995–2008	P 3-h at approx 20 stations	T daily e-obs	binning exponential regression	ERA-Interim 1989–2008
Romania [66]	1951–2014	P 1-h, daily at 9 stations	T daily	binning [32]	Best Lifted Index (four layers)
Romania [85]	1966–2007	rainfall events at 6 stations	T daily	binning [32]	maximum intensity index (IMAX)
South Korea [77]	1980–2014	P 1-h at 26 stations	T 1-h, Tdew 1-h	quantile regression binning with constant bin width binning with constant bin number	humidity, pressure, cloud type
Japan [95]	1951–2010	P 10 min, P 1-h	T monthly	least squares	
Contiguous U.S. [96]	longest 1948–2009 shortest 1948–1986	P 1-h at 14 stations divided in 4 regions	T daily 2 °C	binning method	
Contiguous U.S. [90]	1950–2009	P 1-h at 1029 stations	T daily gridded at 1/16 degree	binning method [32]	
Contiguous U.S. [35]	longest 1948–2009 shortest 1948–1986	P 1-h at 14 stations divided in 4 regions	T daily 2 °C	binning method	
Contiguous U.S. [54]		P 1-h gridded	T 1-h, Tdew 1-h gridded	off-line change point analysis [97]	daily lightning data

4.2. Disaggregation of Precipitation Events

Various methods for the identification of stratiform and convective precipitation have been developed. These methods are usually based on synoptic and/or radar observations and reanalysis, the state of the weather, rain intensity fluctuations, or lightning occurrence [33,43,44,51,54,98]. Thanks to the aforementioned different properties of stratiform and convective components, it is, to some extent, possible to distinguish them directly in precipitation data [99]. It is important to point out that most of the methods listed here have the potential to underestimate the occurrence of convective precipitation, namely the methods based on threshold precipitation intensity. Additionally, the scarcity of stations can underestimate the occurrence of convective events in observed data, e.g., in the case when the convective events are recognized based on observed lightning [54].

A simple rain cell tracking method allows for a separation between stratiform and convective types of precipitation events and reveals a clearly different behavior of their life cycles [100]. SYNOP reports (surface synoptic observations) are the basis of the disaggregation algorithm proposed in [98]. The main advantage of the method is that it is capable of capturing the convective rains of low intensity. On the other hand it needs the full SYNOP reports and it is impossible to use this method on data from automatic stations or on simulations from climate models. Therefore, the application of the method is limited. Basically, the algorithm operates with two criteria: the convective and stratiform precipitation types are characterized by different types of weather events (main criterion) and from different types of clouds (secondary criterion). Another approach based on weather observation data was presented in [51]. The idea is simple: since the heavy convective summer thunderstorms are associated with lightning, lightning is a good proxy for convective precipitation. The idea is supported by reported observations, e.g., in [101]. On the other hand, not all convective precipitation is due to thunderstorms (showers from cumulus clouds not accompanied by lightning occurrence).

Another disaggregation method is based on the relation between the cumulative precipitation and corresponding precipitation intensity [99]. The method uses the observation that this relation is nearly exponential for subdaily time periods. In contrast to the methods described above, it uses in situ rain gauge data only. The method assumes that the stratiform events are weak and long-lived, while convective events are intense and short-term. The light showers of convective origin cannot be captured by the method. The observed anomalies from exponential function are linked to convective systems. In the original study [99], a subset of global surface precipitation data by the World Meteorological Organization was analyzed. The study found that the relation between cumulative precipitation and precipitation intensity has a nearly exponential shape. This approach and the derived method was later used for the Spanish Mediterranean coast and Central Europe [76,102].

To sum up, distinguishing between the convective and stratiform precipitation events is crucial while studying the P-T scaling; the obtained P-T scaling of total precipitation may be unphysically steep due to the prevailing occurrence of stratiform precipitation at lower temperatures while convective precipitation at higher temperatures. However, one has to be aware of the fact that some of the convective events may remain unrecognized, especially when using the methods that are based on threshold intensity [35]. Additionally, due to usually small spatial extent of convective precipitation events, it is possible that many of them are not captured when using sparse station data.

5. Conclusions

Here, the current state of research regarding the P-T scaling in midlatitudes was reviewed based on observational studies. The main drivers for the observed super-CC scaling, sub-CC scaling, and negative scaling were described and summarized. It is possible to recognize two main mechanisms of how increasing temperature can influence precipitation extremes in midlatitudes: increased water content and enhanced atmospheric convection.

The super-CC scaling is linked to convective precipitation in two ways: convective precipitation events are more sensitive to an increase in air temperature and they prevail at higher temperatures; the essential reason for the super-CC scaling is linked to the dynamics of the convective events.

As these two factors are strongly interlinked, deciding on their relative importance is almost impossible. The sub-CC scaling or even negative scaling at very high temperatures was explained by the lack of moisture; however it can be an artifact caused by smaller observation samples underestimating high quantiles.

To obtain robust results it is beneficial to include the scaling with dew point temperature. For understanding physical mechanisms/drivers, it is important to distinguish between convective and non-convective precipitation events to avoid overly steep P-T scaling because the two components behave differently also in terms of scaling with temperature. Further, some of the convective events might remain unrecognized due to principles on which most of the disaggregation methods are based.

Finally, it is essential to keep in mind the objective of a given observational study and establish data homogeneity and proper quality control. Specifically, one should be also aware that shorter observational time series may provide highly uncertain results due to undersampling of very high percentiles which are of interest while studying the P-T scaling of precipitation extremes. Advanced methods, such as quantile regression or extreme value distributions, may improve the estimates of high quantiles, but the length of data still remains a critical issue.

In conclusion, future research efforts should be focused on better understanding convective precipitation, including their links to moisture availability, and better distinguishing between non-convective and convective precipitation events. Both of these research directions need sufficient data sets, which highlights the necessity of improving observational systems and advantages of interconnection of observations and modeling in the research studies focused on the P-T scaling.

Author Contributions: M.M. conceived the idea of the review, prepared the literature summary and drafted the text. J.K. contributed to the structure and focus of the review. Both authors reviewed the manuscript. All authors have read and agreed to the published version of the manuscript.

Funding: The study was supported by the Czech Science Foundation, project no 20-28560S.

Acknowledgments: MM is grateful to Julie Novakova Martinkova, Adela Martinkova, Filip Novak and Jack Regan-Kirwan for unlimited technical, logistic and language support.

Conflicts of Interest: The authors declare no conflict of interest.

Abbreviations

The following abbreviations are used in this manuscript:

CAPE	Convective Available Potential Energy
CC	Clausius-Clapeyron
P-T	precipitation-temperature
SYNOP	surface synoptic observations
THR	threshold temperature

References

1. Held, I.M.; Soden, B.J. Robust responses of the hydrological cycle to global warming. *J. Clim.* **2006**, *19*, 5686–5699.
2. O’Gorman, P.A. Precipitation extremes under climate change. *Curr. Clim. Chang. Rep.* **2015**, *1*, 49–59.
3. Myhre, G.; Alterskjær, K.; Stjern, C.W.; Hodnebrog, Ø.; Marelle, L.; Samset, B.H.; Sillmann, J.; Schaller, N.; Fischer, E.; Schulz, M.; et al. Frequency of extreme precipitation increases extensively with event rareness under global warming. *Sci. Rep.* **2019**, *9*, 1–10.
4. Pall, P.; Allen, M.; Stone, D.A. Testing the Clausius–Clapeyron constraint on changes in extreme precipitation under CO₂ warming. *Clim. Dyn.* **2007**, *28*, 351–363.
5. Allen, M.R.; Ingram, W.J. Constraints on future changes in climate and the hydrologic cycle. *Nature* **2002**, *419*, 228–232.
6. Trenberth, K.E.; Dai, A.; Rasmussen, R.M.; Parsons, D.B. The changing character of precipitation. *Bull. Am. Meteorol. Soc.* **2003**, *84*, 1205–1218.

7. Christensen, J.H.; Christensen, O.B. Climate modelling: severe summertime flooding in Europe. *Nature* **2003**, *421*, 805–806.
8. Sherwood, S.C.; Ingram, W.; Tsushima, Y.; Satoh, M.; Roberts, M.; Vidale, P.L.; O’Gorman, P.A. Relative humidity changes in a warmer climate. *J. Geophys. Res. Atmos.* **2010**, *115*, D09104.
9. Donat, M.G.; Lowry, A.L.; Alexander, L.V.; O’Gorman, P.A.; Maher, N. More extreme precipitation in the world’s dry and wet regions. *Nat. Clim. Chang.* **2016**, *6*, 508–513.
10. Lu, J.; Xue, D.; Gao, Y.; Chen, G.; Leung, L.; Staten, P. Enhanced hydrological extremes in the western United States under global warming through the lens of water vapor wave activity. *NPJ Clim. Atmos. Sci.* **2018**, *1*, 1–9.
11. Nayak, S.; Dairaku, K.; Takayabu, I.; Suzuki-Parker, A.; Ishizaki, N.N. Extreme precipitation linked to temperature over Japan: current evaluation and projected changes with multi-model ensemble downscaling. *Clim. Dyn.* **2018**, *51*, 4385–4401.
12. Hodnebrog, Ø.; Marelle, L.; Alterskjær, K.; Wood, R.; Ludwig, R.; Fischer, E.; Richardson, T.; Forster, P.; Sillmann, J.; Myhre, G. Intensification of summer precipitation with shorter time-scales in Europe. *Environ. Res. Lett.* **2019**, *14*, 124050.
13. Giorgi, F.; Raffaele, F.; Coppola, E. The response of precipitation characteristics to global warming from climate projections. *Earth Syst. Dyn.* **2019**, *10*, 73–89.
14. Morrison, A.; Villarini, G.; Zhang, W.; Scoccimarro, E. Projected changes in extreme precipitation at sub-daily and daily time scales. *Glob. Planet. Chang.* **2019**, *182*, 103004.
15. Oh, S.G.; Sushama, L. Short-duration precipitation extremes over Canada in a warmer climate. *Clim. Dyn.* **2020**, *54*, 2493–2509.
16. Sousa, P.M.; Ramos, A.M.; Raible, C.C.; Messmer, M.; Tomé, R.; Pinto, J.G.; Trigo, R.M. North Atlantic Integrated Water Vapor Transport—From 850 to 2100 CE: Impacts on Western European Rainfall. *J. Clim.* **2020**, *33*, 263–279.
17. Frich, P.; Alexander, L.V.; Della-Marta, P.; Gleason, B.; Haylock, M.; Tank, A.K.; Peterson, T. Observed coherent changes in climatic extremes during the second half of the twentieth century. *Clim. Res.* **2002**, *19*, 193–212.
18. Trenberth, K.E. Changes in precipitation with climate change. *Clim. Res.* **2011**, *47*, 123–138.
19. Westra, S.; Alexander, L.V.; Zwiers, F.W. Global increasing trends in annual maximum daily precipitation. *J. Clim.* **2013**, *26*, 3904–3918.
20. Ribes, A.; Thao, S.; Vautard, R.; Dubuisson, B.; Somot, S.; Colin, J.; Planton, S.; Soubeyroux, J.M. Observed increase in extreme daily rainfall in the French Mediterranean. *Clim. Dyn.* **2019**, *52*, 1095–1114.
21. Li, G.; Harrison, S.P.; Bartlein, P.J.; Izumi, K.; Colin Prentice, I. Precipitation scaling with temperature in warm and cold climates: an analysis of CMIP5 simulations. *Geophys. Res. Lett.* **2013**, *40*, 4018–4024.
22. Stephens, G.L.; Ellis, T.D. Controls of global-mean precipitation increases in global warming GCM experiments. *J. Clim.* **2008**, *21*, 6141–6155.
23. Boucher, O.; Randall, D.; Artaxo, P.; Bretherton, C.; Feingold, G.; Forster, P.; Kerminen, V.M.; Kondo, Y.; Liao, H.; Lohmann, U.; et al. Clouds and aerosols. In *Climate Change 2013: The Physical Science Basis. Contribution of Working Group I to the Fifth Assessment Report of the Intergovernmental Panel on Climate Change*; Cambridge University Press: Cambridge, UK, 2013; pp. 571–657.
24. Allan, R.P.; Liu, C.; Zahn, M.; Lavers, D.A.; Koukouvagias, E.; Bodas-Salcedo, A. Physically consistent responses of the global atmospheric hydrological cycle in models and observations. *Surv. Geophys.* **2014**, *35*, 533–552.
25. Kundzewicz, Z.W. *Changes in Flood Risk in Europe*; CRC Press: Boca Raton, FL, USA, 2019.
26. Madsen, H.; Lawrence, D.; Lang, M.; Martinkova, M.; Kjeldsen, T. Review of trend analysis and climate change projections of extreme precipitation and floods in Europe. *J. Hydrol.* **2014**, *519*, 3634–3650.
27. Sunyer, M.; Hundechea, Y.; Lawrence, D.; Madsen, H.; Willems, P.; Martinkova, M.; Vormoor, K.; Bürger, G.; Hanel, M.; Kriaučiūnienė, J.; et al. Inter-comparison of statistical downscaling methods for projection of extreme precipitation in Europe. *Hydrol. Earth Syst. Sci.* **2015**, *19*, 1827–1847.
28. Lehmann, J.; Coumou, D.; Frieler, K. Increased record-breaking precipitation events under global warming. *Clim. Chang.* **2015**, *132*, 501–515.
29. Hand, W.H.; Fox, N.I.; Collier, C.G. A study of twentieth-century extreme rainfall events in the United Kingdom with implications for forecasting. *Meteorol. Appl.* **2004**, *11*, 15–31.

30. Barbero, R.; Fowler, H.; Lenderink, G.; Blenkinsop, S. Is the intensification of precipitation extremes with global warming better detected at hourly than daily resolutions? *Geophys. Res. Lett.* **2017**, *44*, 974–983.
31. Schroeder, K.; Kirchengast, G. Sensitivity of extreme precipitation to temperature: the variability of scaling factors from a regional to local perspective. *Clim. Dyn.* **2018**, *50*, 3981–3994.
32. Lenderink, G.; Van Meijgaard, E. Increase in hourly precipitation extremes beyond expectations from temperature changes. *Nat. Geosci.* **2008**, *1*, 511–514.
33. Berg, P.; Moseley, C.; Haerter, J.O. Strong increase in convective precipitation in response to higher temperatures. *Nat. Geosci.* **2013**, *6*, 181–185.
34. Ali, H.; Mishra, V. Contrasting response of rainfall extremes to increase in surface air and dewpoint temperatures at urban locations in India. *Sci. Rep.* **2017**, *7*, 1–15.
35. Panthou, G.; Mailhot, A.; Laurence, E.; Talbot, G. Relationship between surface temperature and extreme rainfalls: A multi-time-scale and event-based analysis. *J. Hydrometeorol.* **2014**, *15*, 1999–2011.
36. Fujibe, F. Annual variation of extreme precipitation intensity in Japan: Assessment of the validity of Clausius–Clapeyron scaling in seasonal change. *SOLA* **2016**, *12*, 106–110.
37. Sharma, S.; Mujumdar, P. On the relationship of daily rainfall extremes and local mean temperature. *J. Hydrol.* **2019**, *572*, 179–191.
38. Nayak, S.; Takemi, T. Dependence of extreme precipitable water events on temperature. *Atmósfera* **2019**, *32*, 159–165.
39. Lenderink, G.; Barbero, R.; Loriaux, J.; Fowler, H. Super-Clausius–Clapeyron scaling of extreme hourly convective precipitation and its relation to large-scale atmospheric conditions. *J. Clim.* **2017**, *30*, 6037–6052.
40. Rulfová, Z.; Kyselý, J. Trends of convective and stratiform precipitation in the Czech Republic, 1982–2010. *Adv. Meteorol.* **2014**, *2014*, 647938.
41. Han, X.; Xue, H.; Zhao, C.; Lu, D. The roles of convective and stratiform precipitation in the observed precipitation trends in Northwest China during 1961–2000. *Atmos. Res.* **2016**, *169*, 139–146.
42. Goulden, C.E.; Mead, J.; Horwitz, R.; Goulden, M.; Nandintsetseg, B.; McCormick, S.; Boldgiv, B.; Petraitis, P.S. Interviews of Mongolian herders and high resolution precipitation data reveal an increase in short heavy rains and thunderstorm activity in semi-arid Mongolia. *Clim. Chang.* **2016**, *136*, 281–295.
43. Ye, H.; Fetzner, E.J.; Wong, S.; Lambriksen, B.H. Rapid decadal convective precipitation increase over Eurasia during the last three decades of the 20th century. *Sci. Adv.* **2017**, *3*, e1600944.
44. Chernokulsky, A.; Kozlov, F.; Zolina, O.; Bulygina, O.N.; Mokhov, I.; Semenov, V. Observed changes in convective and stratiform precipitation over Northern Eurasia during the last decades. *Environ. Res. Lett.* **2019**, *14*, 045001.
45. Westra, S.; Fowler, H.; Evans, J.; Alexander, L.; Berg, P.; Johnson, F.; Kendon, E.; Lenderink, G.; Roberts, N. Future changes to the intensity and frequency of short-duration extreme rainfall. *Rev. Geophys.* **2014**, *52*, 522–555.
46. Nissen, K.M.; Ulbrich, U. Increasing frequencies and changing characteristics of heavy precipitation events threatening infrastructure in Europe under climate change. *Nat. Hazards Earth Syst. Sci.* **2017**, *17*, 1177–1190.
47. Houze Jr, R.A. *Cloud Dynamics*; Academic Press: Cambridge, MA, USA, 2014; Volume 104.
48. Alduchov, O.A.; Eskridge, R.E. Improved Magnus form approximation of saturation vapor pressure. *J. Appl. Meteorol.* **1996**, *35*, 601–609.
49. Manola, I.; Van Den Hurk, B.; De Moel, H.; Aerts, J.C. Future extreme precipitation intensities based on a historic event. *Hydrol. Earth Syst. Sci.* **2018**, *22*.
50. Chen, C.; Guerit, L.; Foreman, B.Z.; Hassenruck-Gudipati, H.J.; Adatte, T.; Honegger, L.; Perret, M.; Sluijs, A.; Castellort, S. Estimating regional flood discharge during Palaeocene-Eocene global warming. *Sci. Rep.* **2018**, *8*, 1–8.
51. Molnar, P.; Fatichi, S.; Gaál, L.; Szolgay, J.; Burlando, P. Storm type effects on super Clausius–Clapeyron scaling of intense rainstorm properties with air temperature. *Hydrol. Earth Syst. Sci.* **2015**, *19*, 1753–1766.
52. Schleiss, M. How intermittency affects the rate at which rainfall extremes respond to changes in temperature. *Earth Syst. Dyn.* **2018**, *9*, 955–968.
53. Formayer, H.; Fritz, A. Temperature dependency of hourly precipitation intensities—surface versus cloud layer temperature. *Int. J. Climatol.* **2017**, *37*, 1–10.

54. Ivancic, T.J.; Shaw, S.B. A US-based analysis of the ability of the Clausius-Clapeyron relationship to explain changes in extreme rainfall with changing temperature. *J. Geophys. Res. Atmos.* **2016**, *121*, 3066–3078.
55. Zhang, W.; Villarini, G.; Wehner, M. Contrasting the responses of extreme precipitation to changes in surface air and dew point temperatures. *Clim. Chang.* **2019**, *154*, 257–271.
56. Lenderink, G.; Mok, H.; Lee, T.; Van Oldenborgh, G. Scaling and trends of hourly precipitation extremes in two different climate zones—Hong Kong and the Netherlands. *Hydrol. Earth Syst. Sci.* **2011**, *15*, 3033–3041.
57. Grillakis, M.G.; Koutroulis, A.G. Hydrometeorological Extremes in a Warmer Climate: A Local Scale Assessment for the Island of Crete. In Proceedings of the Multidisciplinary Digital Publishing Institute Proceedings, New York, NY, USA, 15–30 November 2018; Volume 7, pp. 22–29.
58. Sim, I.; Lee, O.; Kim, S. Sensitivity analysis of extreme daily rainfall depth in summer season on surface air temperature and dew-point temperature. *Water* **2019**, *11*, 771.
59. Huang, D.; Yan, P.; Xiao, X.; Zhu, J.; Tang, X.; Huang, A.; Cheng, J. The tri-pole relation among daily mean temperature, atmospheric moisture and precipitation intensity over China. *Glob. Planet. Chang.* **2019**, *179*, 1–9.
60. Salby, M.L. *Physics of the Atmosphere and Climate*; Cambridge University Press: Cambridge, UK, 2012.
61. Rennó, N.O.; Ingersoll, A.P. Natural convection as a heat engine: A theory for CAPE. *J. Atmos. Sci.* **1996**, *53*, 572–585.
62. Lepore, C.; Veneziano, D.; Molini, A. Temperature and CAPE dependence of rainfall extremes in the eastern United States. *Geophys. Res. Lett.* **2015**, *42*, 74–83.
63. Pumo, D.; Carlino, G.; Blenkinsop, S.; Arnone, E.; Fowler, H.; Noto, L.V. Sensitivity of extreme rainfall to temperature in semi-arid Mediterranean regions. *Atmos. Res.* **2019**, *225*, 30–44.
64. Byrne, M.P.; O’Gorman, P.A. The response of precipitation minus evapotranspiration to climate warming: Why the “wet-get-wetter, dry-get-drier” scaling does not hold over land. *J. Clim.* **2015**, *28*, 8078–8092.
65. Lenderink, G.; Van Meijgaard, E. Linking increases in hourly precipitation extremes to atmospheric temperature and moisture changes. *Environ. Res. Lett.* **2010**, *5*, 025208.
66. Busuioc, A.; Birsan, M.V.; Carbutaru, D.; Baci, M.; Orzan, A. Changes in the large-scale thermodynamic instability and connection with rain shower frequency over Romania: verification of the Clausius-Clapeyron scaling. *Int. J. Climatol.* **2016**, *36*, 2015–2034.
67. Blenkinsop, S.; Chan, S.; Kendon, E.; Roberts, N.; Fowler, H. Temperature influences on intense UK hourly precipitation and dependency on large-scale circulation. *Environ. Res. Lett.* **2015**, *10*, 054021.
68. Pumo, D.; Carlino, G.; Arnone, E.; Noto, L.V. Relationship between extreme rainfall and surface temperature in Sicily (Italy). *EPiC Ser. Eng.* **2018**, *3*, 1718–1726.
69. Lenderink, G.; Van Meijgaard, E. Unexpected rise in extreme precipitation caused by a shift in rain type? *Nat. Geosci.* **2009**, *2*, 373.
70. Lochbihler, K.; Lenderink, G.; Siebesma, A.P. The spatial extent of rainfall events and its relation to precipitation scaling. *Geophys. Res. Lett.* **2017**, *44*, 8629–8636.
71. Singh, M.S.; O’Gorman, P.A. Influence of microphysics on the scaling of precipitation extremes with temperature. *Geophys. Res. Lett.* **2014**, *41*, 6037–6044.
72. Haerter, J.O.; Berg, P. Unexpected rise in extreme precipitation caused by a shift in rain type? *Nat. Geosci.* **2009**, *2*, 372–373.
73. Haerter, J.; Berg, P.; Hagemann, S. Heavy rain intensity distributions on varying time scales and at different temperatures. *J. Geophys. Res. Atmos.* **2010**, *115*, D17102.
74. Loriaux, J.M.; Lenderink, G.; De Roode, S.R.; Siebesma, A.P. Understanding convective extreme precipitation scaling using observations and an entraining plume model. *J. Atmos. Sci.* **2013**, *70*, 3641–3655.
75. Moseley, C.; Hohenegger, C.; Berg, P.; Haerter, J.O. Intensification of convective extremes driven by cloud–cloud interaction. *Nat. Geosci.* **2016**, *9*, 748–752.
76. Martinkova, M.; Hanel, M. Evaluation of relations between extreme precipitation and temperature in observational time series from the Czech Republic. *Adv. Meteorol.* **2016**, *2016*, 2975380.
77. Park, I.H.; Min, S.K. Role of convective precipitation in the relationship between subdaily extreme precipitation and temperature. *J. Clim.* **2017**, *30*, 9527–9537.
78. Singleton, A.; Toumi, R. Super-Clausius-Clapeyron scaling of rainfall in a model squall line. *Q. J. R. Meteorol. Soc.* **2013**, *139*, 334–339.

79. Berg, P.; Haerter, J.; Thejll, P.; Piani, C.; Hagemann, S.; Christensen, J. Seasonal characteristics of the relationship between daily precipitation intensity and surface temperature. *J. Geophys. Res. Atmos.* **2009**, *114*, D18102.
80. Siler, N.; Roe, G. How will orographic precipitation respond to surface warming? An idealized thermodynamic perspective. *Geophys. Res. Lett.* **2014**, *41*, 2606–2613.
81. Utsumi, N.; Seto, S.; Kanae, S.; Maeda, E.E.; Oki, T. Does higher surface temperature intensify extreme precipitation? *Geophys. Res. Lett.* **2011**, *38*, L16708.
82. Prein, A.F.; Rasmussen, R.M.; Ikeda, K.; Liu, C.; Clark, M.P.; Holland, G.J. The future intensification of hourly precipitation extremes. *Nat. Clim. Chang.* **2017**, *7*, 48–52.
83. Chan, S.C.; Kendon, E.J.; Roberts, N.M.; Fowler, H.J.; Blenkinsop, S. Downturn in scaling of UK extreme rainfall with temperature for future hottest days. *Nat. Geosci.* **2016**, *9*, 24–28.
84. Drobinski, P.; Alonzo, B.; Bastin, S.; Silva, N.D.; Muller, C. Scaling of precipitation extremes with temperature in the French Mediterranean region: What explains the hook shape? *J. Geophys. Res. Atmos.* **2016**, *121*, 3100–3119.
85. Busuioc, A.; Baci, M.; Breza, T.; Dumitrescu, A.; Stoica, C.; Baghina, N. Changes in intensity of high temporal resolution precipitation extremes in Romania: implications for Clausius–Clapeyron scaling. *Clim. Res.* **2017**, *72*, 239–249.
86. Schroeder, K.; Kirchengast, G.; O, S. Strong dependence of extreme convective precipitation intensities on gauge network density. *Geophys. Res. Lett.* **2018**, *45*, 8253–8263.
87. Boessenkool, B.; Brüger, G.; Heistermann, M. Effects of sample size on estimation of rainfall extremes at high temperatures. *Nat. Hazards Earth Syst. Sci.* **2017**, *17*, 1623–1629.
88. Hardwick Jones, R.; Westra, S.; Sharma, A. Observed relationships between extreme sub-daily precipitation, surface temperature, and relative humidity. *Geophys. Res. Lett.* **2010**, *37*.
89. Blenkinsop, S.; Fowler, H.J.; Barbero, R.; Chan, S.C.; Guerreiro, S.B.; Kendon, E.; Lenderink, G.; Lewis, E.; Li, X.F.; Westra, S.; et al. The INTENSE project: using observations and models to understand the past, present and future of sub-daily rainfall extremes. *Adv. Sci. Res.* **2018**, *15*, 117–126.
90. Mishra, V.; Wallace, J.M.; Lettenmaier, D.P. Relationship between hourly extreme precipitation and local air temperature in the United States. *Geophys. Res. Lett.* **2012**, *39*, L16403.
91. Wasko, C.; Sharma, A. Steeper temporal distribution of rain intensity at higher temperatures within Australian storms. *Nat. Geosci.* **2015**, *8*, 527–529.
92. Jenkinson, A.; Collison, F. *An Initial Climatology of Gales Over the North Sea*; Number 62 in Synoptic Climatology Branch Memorandum, Meteorological Office: Bracknell, UK, 1977.
93. Berg, P.; Haerter, J. Unexpected increase in precipitation intensity with temperature—A result of mixing of precipitation types? *Atmos. Res.* **2011**, *119*, 56–61.
94. Drobinski, P.; Da Silva, N.; Panthou, G.; Bastin, S.; Muller, C.; Ahrens, B.; Borga, M.; Conte, D.; Fosser, G.; Giorgi, F.; et al. Scaling precipitation extremes with temperature in the Mediterranean: past climate assessment and projection in anthropogenic scenarios. *Clim. Dyn.* **2018**, *51*, 1237–1257.
95. Fujibe, F. Clausius–Clapeyron-like relationship in multidecadal changes of extreme short-term precipitation and temperature in Japan. *Atmos. Sci. Lett.* **2013**, *14*, 127–132.
96. Shaw, S.B.; Royem, A.A.; Riha, S.J. The relationship between extreme hourly precipitation and surface temperature in different hydroclimatic regions of the United States. *J. Hydrometeorol.* **2011**, *12*, 319–325.
97. Basseville, M.; Nikiforov, I.V. *Detection of Abrupt Changes: Theory and Application*; Prentice Hall: Englewood Cliffs, NJ, USA 1993; Volume 104.
98. Rulfová, Z.; Kyselý, J. Disaggregating convective and stratiform precipitation from station weather data. *Atmos. Res.* **2013**, *134*, 100–115.
99. Tremblay, A. The stratiform and convective components of surface precipitation. *J. Atmos. Sci.* **2005**, *62*, 1513–1528.
100. Moseley, C.; Berg, P.; Haerter, J.O. Probing the precipitation life cycle by iterative rain cell tracking. *J. Geophys. Res. Atmos.* **2013**, *118*, 13–361.

101. Yair, Y.; Lynn, B.; Price, C.; Kotroni, V.; Lagouvardos, K.; Morin, E.; Mugnai, A.; Llasat, M.d.C. Predicting the potential for lightning activity in Mediterranean storms based on the Weather Research and Forecasting (WRF) model dynamic and microphysical fields. *J. Geophys. Res. Atmos.* **2010**, *115*.
102. Ruiz-Leo, A.M.; Hernández, E.; Queralt, S.; Maqueda, G. Convective and stratiform precipitation trends in the Spanish Mediterranean coast. *Atmos. Res.* **2013**, *119*, 46–55.



© 2020 by the authors. Licensee MDPI, Basel, Switzerland. This article is an open access article distributed under the terms and conditions of the Creative Commons Attribution (CC BY) license (<http://creativecommons.org/licenses/by/4.0/>).